Research of Materials Science
Volume 7, 2021, PP. 1-7

Magnetic Defect in Phosphorene Nanoribbons

Qimin Cheng [1], Wei Sheng [1], Lingxi Wu [1], Chun Hu[1]

1.School of Physics and Electronic Science, Hunan University of Science and Technology, Xiangtan, Hunan 411201, China

†Email: shengwei@hnust.edu.cn; Lwxu@hnust.edu.cn

Abstract

Two dimensional few-layer black phosphorus crystal structures have recently been fabricated and have demonstrated great potential in electronic applications. Defects are inevitably present in materials and always can affect their properties. In this work, we employed first principles density functional theory calculations to study the quantum confinement effects on the electronic properties of the phosphorene nanoribbons (PNR)single and double SV- (5/9) vacancy defects. We find that these defects are all created quite easily in phosphorene nanoribbons. We find that these defects are all quite easily to deal with in phosphorene with higher areal density. With SV (5/9) existing, introduces unoccupied localized states into phosphorene's fundamental band gap half metal character, close the band gap and causing a turning from semiconductor to conductor, which are verified with Band structure picture or Projected density of states and all these disparities due to the atom which possesses one suspension bond. Specifically, the Sv-(5/9) can introduce unoccupied localized states into phosphorene's fundamental band gap.

Keywords: Phosphorene Nanoribbons; Defect State; First Principles Calculation; Electronic Structure; Magnetic Materials

1 INTRODUCTION

In recent years, a large number of high-quality monomer phosphorene nanoribbons have been produced by ion cutting macro black phosphorus crystals, which will lead to a new trend in the research of black phosphorus nanoribbons. Since graphene was first stripped from graphite in 2004, ultra-thin two-dimensional materials have played an important role in the whole material research and have been widely used. In the past ten years, the key member phosphorene has shown a wealth of physical, chemical and mechanical properties.

1.1 Research Background and Properties of Phosphorene

Phosphorene is a two-dimensional structure material, which is composed of phosphorus atoms arranged in high and low layers, and finally forms a two-dimensional structure material with armchair direction and zigzag direction perpendicular to each other. The preparation technology of graphene has been greatly promoted and widely studied since graphene was stripped experimentally. In recent years, the process of two-dimensional black phosphorus stripping from the experiment has been gradually mature compared with a large number of laboratories at home and abroad have used phosphorene samples for research through cooperation. At present, some studies have shown that black phosphorus system has very small elastic modulus, so it has high carrier mobility. In addition, single-layer phosphorene has a hole mobility of $10\sim26\times10^3 cm^2V^{-1}s^{-1}$.

1.2 Background and Properties of Phosphorene Nanoribbons

In phosphorene nanoribbons, the electronic properties show that the top and bottom of the valence band are contributed by the atoms in the band. The band gap of the phosphorene nanoribbons decreases with the increase of the bandwidth. The band gap of the serrated phosphorene nanoribbons is almost twice that of the armchair shaped. If a transverse electric field of about 7V / M is applied from the top to the bottom of the gate, a channel with a break ratio of 103 will appear, which proves the on-state stability of FET. All phosphorus-based field effect transistor avoids the interface contact effect between metal and semiconductor region. The edge hydrogen passivation makes the zigzag phosphorene nanoribbons change from indirect band gap to direct band gap and enlarge the band gap. For armchair shaped phosphorene nanoribbons, the edge state indicates that this will eventually lead to the disappearance

of metallicity, resulting in the transition from metal to semiconductor.

The electrical and magnetic properties of serrated phosphorene nanoribbons can be effectively controlled by passivation of different elements. The electronic and magnetic properties of these As and Sb zigzag phosphorene nanoribbons will also be helpful for their future applications in nanoelectronics and spintronics.

1.3 The Main Research Contents of This Paper

Using density functional theory and molecular dynamics calculation, the stability and electronic structure of typical point defects in one-dimensional semiconductor phosphorene nanoribbons have been systematically studied. In this study, hydrogen atom was chosen to passivate the phosphorene nanoribbons, and the effects of various local defects on the phosphorene were studied. Firstly, the hydrogen passivation of the armchair and zigzag phosphorene nanoribbons with different lattice constants is optimized to a given precision, and the nanostructure with the lowest total energy is selected as the selection system for the next step of calculation. The armchair and zigzag nanoribbons were expanded for several cycles, and the same type of defects were added respectively. The structure of the defect phosphorene nanoribbons was further calculated. According to the obtained molecular data, the density of States, energy band structure, charge distribution and spin density distribution images were drawn. The information was obtained by analyzing the images, and the conclusion was obtained by combining the theoretical prediction with the properties of materials.

1.4 Theoretical Calculation Principles and Tools

Our first principles calculations based on density Functional Theory (DFT) were performed using a package (VASP). The ion - electron interaction is described by the projected enhanced wave method (PAW). The generalized gradient approximation (PBE) proposed by Perdew, Burke, and Ernzerhof is used. The cutoff energy was set to 500eV, and the Brillouin region was sampled using K point monkhorst-Pack grid and 3×3×1 point. Meanwhile, a vacuum layer of 10A is used in the Z direction to avoid the interaction between adjacent planes. When the lattice optimizes the atomic position until the force is less than 0.01eV/ A. The convergence criterion for energy in a self-consistent process is set to 10^{-5}eV.

2 GEOMETRIC AND ELECTRONIC PROPERTIES OF HYDROGEN PASSIVATED PHOSPHORENE NANORIBBONS

2.1 Geometric Properties of Hydrogen Passivated Phosphorene Nanoribbons

Based on the armchair and zigzag structure of phosphorene, the phosphorene nanoribbons and hydrogen passivated phosphorene nanoribbons, the phosphorene nanoribbons with different position defects and the phosphorene nanoribbons with the same defects in different positions are used as the research objects in this paper. The conjugate gradient algorithm is used to complete the structural relaxation of all atomic coordinates until the total energy and atomic force converge to 10-5ev and 0.01ev/Å, respectively. Finally, the lattice parameters of phosphorene are calculated as a15 (P) = 4.15 Å, a16 (P) = 4.16 Å, z22 (P)=29 Å and z24 (P) = 3.30 Å and the vacuum space in Z direction is 10 Å. The truncation energy is set to 500 EV in the calculation parameters, and the Brillouin zone is sampled by 3 × 3 regular grid.

Figure 1 shows (a) armchair phosphine nanoribbons with a length of 16 atoms, (b) armchair phosphine nanoribbons with a length of 15 atoms, (c) zigzag phosphorene nanoribbons with a length of 24 atoms, and (d) zigzag phosphorene nanoribbons with a length of 22 atoms. The purple and white spheres represent the P (phosphorus) and H (hydrogen) atoms, respectively. N is the length of phosphorene nanoribbons. The gray dotted line indicates the periodic repeated lattice boundary of the phosphorene nanoribbons.

2.2 Electronic Structure of Hydrogen Passivated Phosphorene Nanoribbons

In this study, hydrogen passivated phosphorene nanoribbons, which are the most widely used, were selected as the basic research model. Two paths of phosphorene nanoribbons are calculated, which correspond to the zigzag direction and armchair direction respectively. For any direction, the highly symmetric structure and the sub high

symmetry structure of P atom are separately put into calculation by different band width N(odd or even). Each hydrogen passivated phosphorene nanoribbons used in this study are still indirect band gap semiconductors, Even if they show different symmetries.

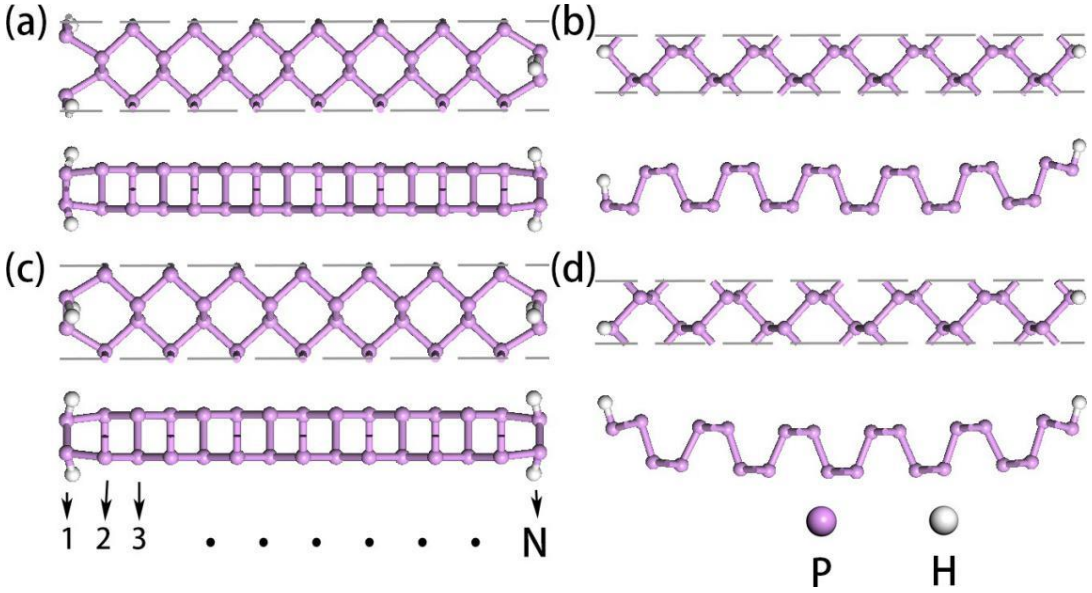


FIGURE 1. PERIODIC STRUCTURE OF PHOSPHORENE NANORIBBONS WITH HYDROGEN PASSIVATION EDGES (TOP AND SIDE VIEWS)

2.2 Electronic Structure of Hydrogen Passivated Phosphorene Nanoribbons

In this study, hydrogen passivated phosphorene nanoribbons, which are the most widely used, were selected as the basic research model. Two paths of phosphorene nanoribbons are calculated, which correspond to the zigzag direction and armchair direction respectively. For any direction, the highly symmetric structure and the sub high symmetry structure of P atom are separately put into calculation by different band width N(odd or even). Each hydrogen passivated phosphorene nanoribbons used in this study are still indirect band gap semiconductors, even if they show different symmetries.

The contribution of hydrogen atoms to the total Density of states is very small and negligible compared with many phosphorus atoms. Therefore, the total density of states images of phosphorene nanoribbons affected by hydrogen passivation are more obvious in the total Density of states. The density of states of all the structures has no peak near the Fermi level, and the peaks of all structures are concentrated in a distance from the Fermi level, and the band gap is about 0.8eV. Even if the symmetry is different, the density of states between the zigzag and armchair shaped phosphorene nanoribbons will have an obvious similarity. The peak value of the density of states in the main region of the density of states of the phosphorene nanoribbons with symmetrical upper and lower edges is higher than that of the asymmetric structure. This shows that the wave function of the upper and lower edges of the phosphorene nanoribbons makes the density of states stack at the same wavelength.

3 GEOMETRIC AND ELECTRONIC PROPERTIES OF HYDROGEN PASSIVATED PHOSPHORENE NANORIBBONS WITH DEFECTS

3.1 Geometric Properties of Hydrogen Passivated Phosphorene Nanoribbons

The hydrogen passivated phosphorene nanoribbons were expanded for seven cycles in the zigzag direction and five cycles in the armchair direction. Sv (5|9) defects were added at the edge and center respectively, and the hydrogen passivated phosphorene nanoribbons with double symmetrical defects were fabricated.

3.2 Analysis of Electron Spin Density

The stability and electronic properties, including formation energy, total magneton and band gap, of the original and

defective phosphorene were calculated. As expected, according to the formation energy data in table 4.1, these defect containing phosphorene nanoribbons are easy to form, and the results also show that, with the defect concentration increasing, the formation energy increased linearly.

Table 1 shows the stability and electronic properties of all intact and defective phosphorene nanoribbons, including formation energy (eV), total magnetic moment (μ b) and band gap (eV). The formation energy of defects on hydrogen passivated phosphorene nanoribbons is the highest when there is only one defect, and when the second defect is to be formed. The required formation energy will be reduced. In the case of normal defect formation, sometimes the band gap will be zero, because the defect enters the local quantum state, locates at the Fermi level in the energy band, and passes through the Fermi level or is very close to the Fermi level. SV (5|9) makes hydrogen passivated zigzag phosphorene nanoribbons and hydrogen passivated armchair phosphine nanoribbons produce nearly one Bohr magneton, which has little effect on the movement of defects. Moreover, with the increase of concentration, the magneton of the phosphorene nanoribbons containing Sv (5|9) defects will increase directly. Even if the vacancy is formed near the edge, the levitation bond atoms are also on the edge of combining with other H atoms with different structures, which does not cause the degradation of magnetization, but distributes the magnetization to the adjacent atoms.

The special energy band of the defect state in the system will become closer to Fermi level as the defect position gradually shifts to the center of the nanoribbons. Finally, in the armchair shaped phosphine nanoribbons with asymmetric structure, the defect is located in the center of the nanoribbons and reaches the position of crossing the Fermi level. However, in the zigzag phosphorene nanoribbons, the defect states have merged and crossed the Fermi level at the edge of the asymmetric type, while in other zigzag phosphorene nanoribbons, the defect states always stay at a certain distance from the Fermi level.

3.3 Band Structure, Density of States and Comprehensive Analysis

In the case of haploid defects, the closer the defect is to the edge of the nanoribbons, the higher the density of states peak. It can be seen from table 1 that the closer the defect is to the edge, the lower the required formation energy. Once the defect is formed, a fixed amount of magnetic moment will be introduced into the system, therefore, it is more reasonable to set the defects on the edge of the nanoribbons. Although the formation energy of the defect on the chair shaped phosphorene nanoribbons is higher than that of the zigzag shape, the increase of the density of states caused by the defect marginalization is greater, so it has greater value.

TABLE 1 STABILITY AND ELECTRONIC PROPERTIES OF ALL INTACT AND DEFECTIVE PHOSPHORENE NANORIBBONS CALCULATED

	E_F（eV）	Mag（μ_B）	E_g（eV）
a15-SV（5|9）-a	-1.188	0.999	1.018
a15-SV（5|9）-b	-1.615	0.934	1.075
a15-SV（5|9）-c	-1.577	0.961	1.032
a15-SV（5|9）-d	-1.615	0.934	1.069
a16-SV（5|9）-e	-1.175	1.000	1.017
a16-SV（5|9）-f	-1.614	0.934	0.000
z22-SV（5|9）-g	-1.314	0.979	0.000
z22-SV（5|9）-h	-1.596	0.993	1.284
z22-SV（55|66）-i	-2.032	0.000	1.222
z22-SV（5|9）-j	-1.596	0.993	1.280
z24-SV（5|9）-k	-1.561	0.992	1.236
z24-SV（5|9）-l	-1.620	0.994	1.257
a15-DV（5|9）-m	-2.936	1.934	1.139
z24-DV（5|9）-n	-3.130	2.000	1.231
z24-DV（5|9）-o	-3.198	1.962	1.238

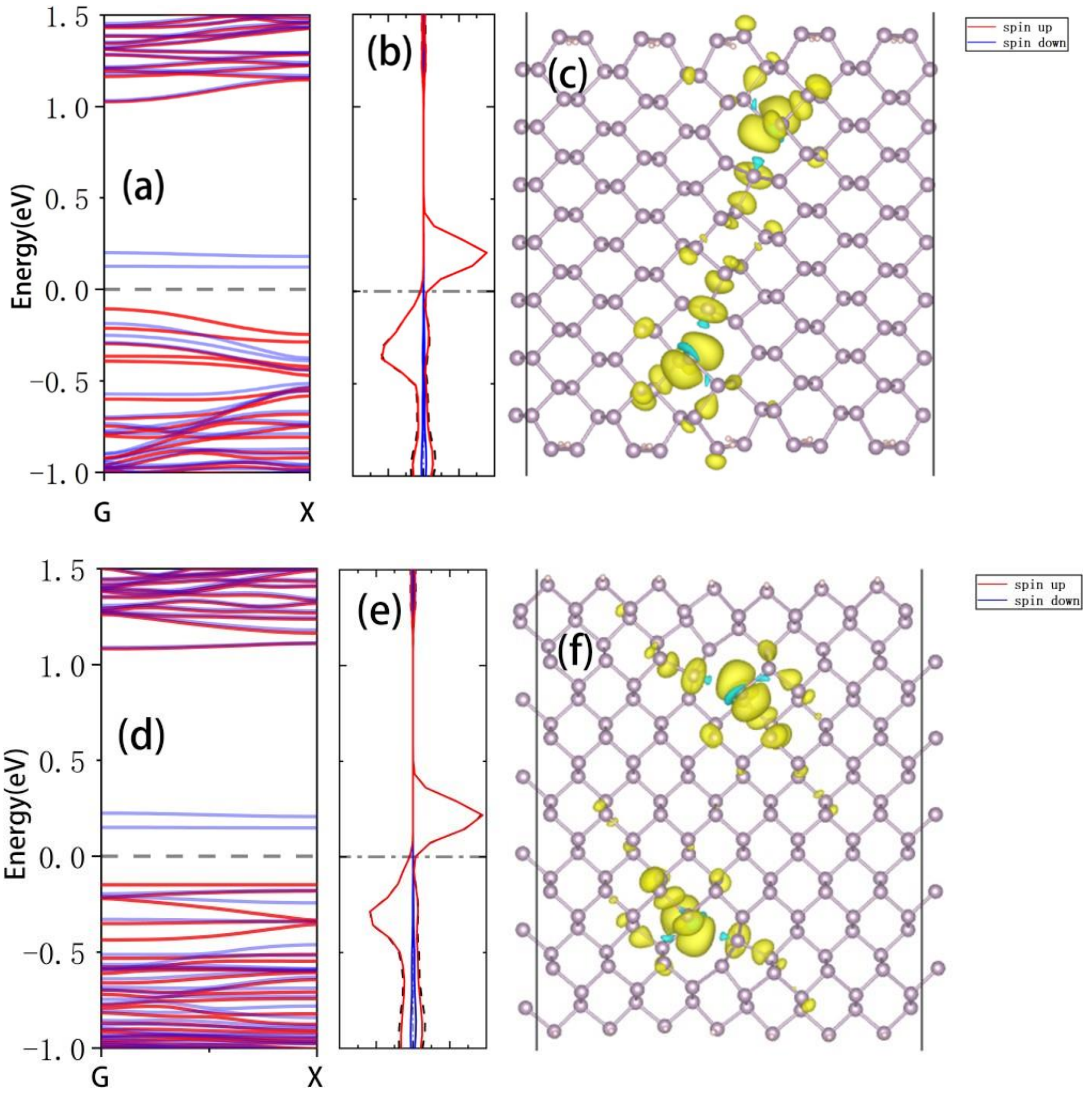


FIGURE 2. BAND STRUCTURE, DENSITY OF STATES, AND PERIODIC STRUCTURE AFTER HYDROGEN PASSIVATION

Figure 2 shows (a) the energy band structure of hydrogen passivated a15-DV (5|9)-m, (d) the band structure of hydrogen passivated z24-DV (5|9)-n. the semitransparent red line and the translucent blue line represent the spin up and spin down energy bands respectively. The sum of the comprehensive projected densities of states and the total densities of states of all the observable magneton atoms shown in the middle panel (b) and (E) correspond to the blue lines, red lines and black dotted lines of the s-orbital, p-orbital and the total Density of states. And (c) a15-DV (5|9)-m, (f) z24-DV (5|9)-n structure. The vertical axis energy scale is marked in units of 0.5 from negative 1.0 to positive 1.5. The unit is electron volt. The path of K point on the horizontal axis is from G point to x point. The Fermi energy level is marked with gray dotted line and set on the zero scale. In Fig. 2, the changes of the band structure, density of states and spin density images of the material system are described in Fig. 2 when the defect concentration is not increased in the periodic direction, but is doubled in the direction perpendicular to the period. Because the levitation bond is located at the center of the spin density of each conventional Sv (5|9) defect structure and contributes most of the polarizability. The existence and influence of dangling bond is considered to be the key to the unique characteristics of SV (5|9). The richness, band structure and density of states (DOS) of SV (5|9) reflect the excellent properties of SV (5|9). As shown in Fig. 2 (a), in the energy band structure calculation, the defect state with spin down is introduced above the Fermi energy. Changing the position of the defect can well induce and adjust the position of the defect state, and the increase of the injection concentration will obviously promote the energy band to move towards the Fermi energy direction. The middle panel shows the total projected density of states of selected atoms P3, P8, P23, P48, P62 and P117. Through the above research, it is concluded that although several atoms have abnormal fractional density of states, a high percentage of the specific peaks are still contributed by the suspended

bond atoms.

It can be seen from Fig. 2 (a) and Fig. 2 (d) that when the concentration of defects in the longitudinal direction increases, the number of corresponding special energy bands will also double. After doubling, the energy bands on the same side of Fermi level do not coincide directly, but they are distributed up and down at the place not far from Fermi level on one side of Fermi level. In table 4.1 of this paper, it is not considered that the band gap is greatly reduced, however, if the defect energy level can make the material system show a small band gap of about 0.2eV in other special applications, it will be different, but this situation is not taken into account. According to the description of the density of states in Fig. 2 (b) and Fig. 2 (e), the defect structures in the two directions show similar properties in the density of states. At the same time, according to Fig. 2 (c) and Fig. 2 (f), the similarity between the band structure and the density of States is due to the eccentric position of the non extreme edge of the longitudinally symmetric defect, so that the properties of the hanging bond can be fully reflected in Fig. 2

For the calculation of formation energy, the following formula is used:

$$EF = E_{\text{perfect}} - E_{\text{defective}} - \text{n} * E_{\text{perP}}$$

The formation energy in this study is calculated according to the above formula, where $E_{perfect}$ is the corresponding direction and step of the total energy of the original structure of H passivation, $E_{deffective}$ is the H-passivated phosphorene nanoribbons, E_{perP} is the total energy of each P atom, and n is the number of defects in each repetition.

4 CONCLUSIONS

The geometric structures of a15-SV (5|9)-A and other defective phosphorene nanoribbons in 5-cycle and 7-cycle supercell have been systematically studied. The DFT of VASP is used to analyze it. It is found that SV-(5|9) defects are easily generated in the phosphorene nanoribbons compared with graphene nanoribbons and silene nanoribbons, and can be stably retained in all these types of graphene nanoribbons. Defects with different structures exhibit different stability and electronic structures in phosphine. For the two kinds of phosphorene nanoribbons, the closer the defect is to the edge, the lower the required formation energy is. Once the defect is formed, a fixed amount of magnetic moment will be introduced into the system. Therefore, it is more reasonable to set the defect at the edge of the nanoribbons. Although the formation energy of the defect on armchair type phosphorene nanoribbons is higher than that of the zigzag shape, however, the increase of density of states caused by defect marginalization is greater, so it has greater value. The eccentric position of the non-extreme edge of the longitudinal symmetric defect makes the properties of the hanging key fully reflected. In the presence of SV - (5|9), the unoccupied local state will be introduced into the base band gap of phosphorene, which will bring half gold property and close the band gap, which will lead to the transition from semiconductor to conductor. This is verified in the energy band structure diagram and the density of states diagram. In particular, SV -(5|9) and SV - (55|66) defects can induce hole doping of phosphorene. However, SV -(5|9) defects can lead to the local magnetic moments of all the phosphorene nanoribbons. The theoretical calculation of this study provides an important insight into the recognition of point defects in subsequent experiments and the understanding of their effects on the electronic properties and potential applications of phosphorene.

REFERENCES

[1] Novoselov K S, Jiang D, Schedin F, et al. Two-dimensional atomic crystals[J]. Proceedings of the National Academy of Sciences, 2005, 102（30）:10451-10453.

[2] Kar M, Sarkar R, Pal S, et al. Edge Modified Phosphorene Antidot Nanoflakes and Their van der Waals.

[3] Heterojunctions for Solar Cell Applications[J]. The Journal of Physical Chemistry C, 2019, 123（34）.

[4] Osada M, Sasaki T. Two-Dimensional Dielectric Nanosheets: Novel Nanoelectronics From Nanocrystal Building Blocks[J]. Advanced Materials, 2012, 24(2): p.210-228.

[5] Xu M, Liang T, Shi M, et al. Graphene-Like Two-Dimensional Materials[J]. Chemical Reviews, 2013, 113（5）:3766-3798.

[6] Geim A K, Novoselov K S. The rise of graphene[J]. Nature Materials, 2007, 6（3）:183-191.

[7] Liu Y C, Ren H T, Gao P F, et al. Flexible modulation of electronic and magnetic properties of zigzag H-MoS2 nanoribbons by crack defects[J]. Journal of Physics Condensed Matter, 2018, 30（28）:285302-.
[8] Watanabe K, Taniguchi T, Kanda H. Direct-bandgap properties and evidence for ultraviolet lasing of hexagonal boron nitride single crystal[J]. Nature Materials, 2004, 3（6）:404-409.
[9] Radisavljevic B, Radenovic A, Brivio J, et al. Single-layer MoS2 transistors[J]. Nature Nanotechnology, 2011, 6（3）:147-150.
[10] Hu W, Li Z, Yang J. Structural, electronic, and optical properties of hybrid silicene and graphene nanocomposite[J]. Journal of Chemical Physics, 2013, 139（15）:154704.
[11] Kresse G, Jü. Hafner. Ab Initio Molecular Dynamics for Liquid Metals[J]. Physical review. B, Condensed matter, 1993, 47（1）:558-561.
[12] Liu Y, Xu F, Zhang Z, et al. Two-Dimensional Mono-Elemental Semiconductor with Electronically Inactive Defects: The Case of Phosphorus[J]. Nano Letters, 2014, 14（12）:6782.
[13] Leenaerts O, Partoens B, Peeters F M. Graphene: A Perfect Nanoballoon[J]. Applied Physicsletters, 2008, 93（19）:267-269.
[14] John P. Perdew, Kieron Burke, Matthias Ernzerhof. Generalized Gradient Approximation Made Simple[J]. Physical Review Letters, 1996.

AUTHORS



[1] 成起民（1996-），男，汉族，湖南科技大学物理与电子科学学院研究生，研究方向为第一性原理研究二维材料，Email：2303679399@qq.com